

# Seeding effect in hydrothermal synthesis of nanosize yttria

PRAMOD K. SHARMA, M. H. JILAVI, R. NAß, H. SCHMIDT

Institut fuer Neue Materialien, Gebaeude 43, Im Stadtwald, D-66123 Saarbrucken, Germany

Nanoscale particles are of interest in fundamental as well as applied research because many properties of materials change drastically when the crystallite size reaches the nano/submicrometer range [1]. Since nanoscale particles have relatively large surface areas, they tend to agglomerate to minimize the total surface energy. Agglomeration adversely affects their properties. One approach to make nanoscale particles without agglomeration involves the use of surfactant molecules during the synthesis stage [2]. The surfactant molecules adsorb on the surface of particles and stabilize the particle against agglomeration by either electrostatic repulsion or steric force [3]. This is one of the chemical approaches to control the particle size. It has been demonstrated that the physical properties, especially particle size and surface area of ceramic powders can be altered by adopting a combination of two processes, namely coprecipitation and hydrothermal. Beidellite  $\text{Na}_{0.4}\text{Al}_2(\text{Si}_{3.6}\text{Al}_{0.4})\text{O}_{10}(\text{OH})_2 \cdot 4\text{H}_2\text{O}$  has been synthesized by a combination of sol-gel and hydrothermal processes, in which an ideal beidellite composition was prepared from either tetra ethyl orthosilicate (TEOS) [4] or colloidal silica [5]. Yanazisawa *et al.* [6] used the combination of coprecipitation and hydrothermal methods to obtain beidellite at a lower temperature without agglomeration.

Recently, it has been reported that the formation of many transition metal oxides, e.g.,  $\text{Fe}_3\text{O}_4$ ,  $\text{Fe}_2\text{O}_3$  and  $\alpha\text{-Al}_2\text{O}_3$  may be controlled by nucleating or "seeding" with, e.g.,  $\text{CuO}$ ,  $\text{SiO}_2$  and  $\alpha\text{-Al}_2\text{O}_3$ , respectively [7–9]. Applying the seeding effect in order to enhance transformation kinetics and to control the development of a desired phase has been successfully investigated [9–11]. However, to our knowledge it has not been applied to yttria or doped yttria. The aim of this paper is to report the preparation of nanoscale yttria by a combined method of coprecipitation and hydrothermal processes in the presence of a seed. The coprecipitation method was employed to produce a gel in the presence of modifier (a mixture of tween-80 and  $\beta$ -alanine). Seeds of  $\text{Y}_2\text{O}_3$  were added to the coprecipitated gel. The gel was then subjected to a hydrothermal treatment. This study showed that the seeding not only represents a unique method to obtain nanosize yttria but also prevents the formation of hydroxide during the course of hydrothermal treatment. However, the seeding effect was found to be selective of the precursor of yttria.

A precursor solution was prepared by dissolving a known amount of precursor salt ( $\text{Y}(\text{NO}_3)_3 \cdot 5\text{H}_2\text{O}$  or  $\text{YCl}_3 \cdot 4\text{H}_2\text{O}$ ) in water and stirring for 2 h. The

modifier solution was prepared by dissolving 10% wt/wt of the surface modifier with respect to  $\text{Y}_2\text{O}_3$  in 50 ml of an aqueous ammonium hydroxide solution ( $\text{pH} > 10$ ) and stirring for an hour at room temperature. The precursor solution was then added to the modifier solution drop-by-drop through a burette at a controlled rate (10 drops per minute) with vigorous stirring. Seeds of 4% wt/wt of  $\text{Y}_2\text{O}_3$  particles were added to the gel. The hydrothermal treatment of the gel was carried out at  $190^\circ\text{C}$  for 1, 2 and 4 h in a  $300\text{ cm}^3$  stainless steel autoclave lined with Teflon (Bergohof GmbH, Labortechnik; DAH904, Germany). The pressure inside the autoclave was not controlled. However, the autoclave was tight and it is felt that the pressure corresponded to the autogenous water vapour pressure. The resulting powder was washed by 20% acetic acid solution in water and dried in an oven at  $60^\circ\text{C}$  for 24 h.

The bulk density of the material was measured using a Micromeritics densitometer (Accu Pyc 1330). The infrared spectra of the samples were recorded on a Fourier transform infrared spectrometer (Brucker, IFS 25). The surface area was measured by applying multipoint Brunauer–Emmett–Teller (BET) for all samples with a minimum of 5 points on a Micromeritics Unit (ASAP 2400). Powders were degassed at  $150^\circ\text{C}$  before surface area measurements. The crystalline phase was determined by powder X-ray diffraction (XRD) on a D-500 Siemens powder diffractometer. The microstructure of particles was investigated in a high resolution transmission electron microscope (HRTEM) (Philips, CM 200, FEG) operated at 200 kV with a line resolution of 0.14 nm. For the preparation of the TEM specimen, the powder was heavily diluted with acetone, partially deagglomerated by ultrasonic

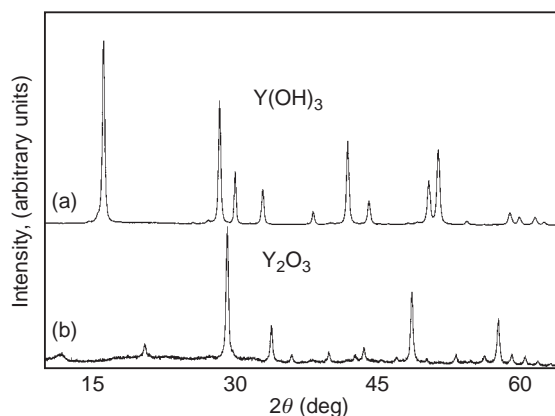


Figure 1 X-ray diffraction patterns of powder derived from (a)  $\text{Y}(\text{NO}_3)_3$  and (b)  $\text{YCl}_3$  precursor in the presence of a seed.

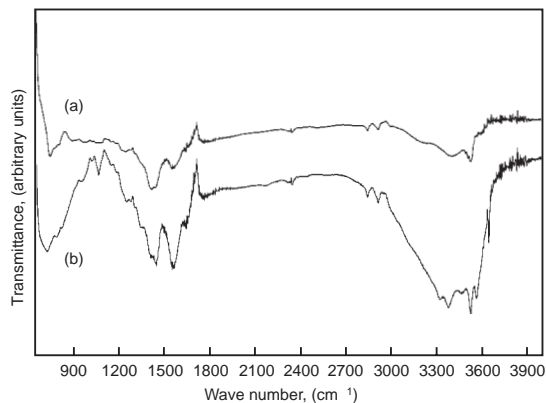


Figure 2 FTIR spectrum of powder derived from (a)  $\text{YCl}_3$  and (b)  $\text{Y}(\text{NO}_3)_3$  precursor in the presence of a seed.

waves and directly spread over a copper grid. The TEM specimen was coated with a very thin carbon layer in order to prevent the charge effect during the microscopy process.

The XRD method was used to determine the phase purity. The powder synthesized from yttrium chloride in the presence of a seed has a structure identical to yttrium oxide as shown in Fig. 1. On the other hand, the powder derived from yttrium nitrate precursor was found to be different from the one

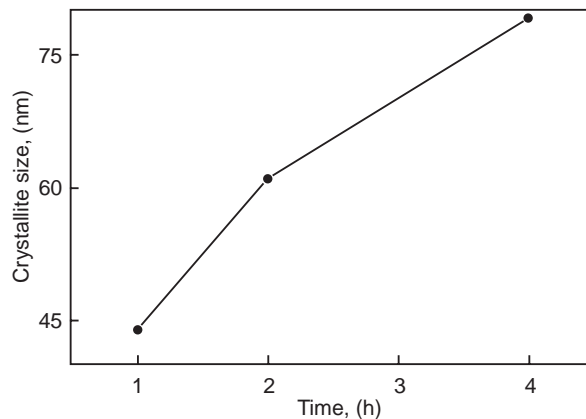


Figure 3 Effect of reaction time on the crystallite size of yttria powder derived from  $\text{YCl}_3$  in the presence of a seed.

obtained by yttrium chloride and its XRD pattern represented a yttrium hydroxide phase. The hydroxide phase was also obtained when the powder was synthesized from yttrium chloride in the absence of a seed. This indicates that a precursor and seeding induce coprecipitation of different phase structures. The role and mechanism of chloride in obtaining a particular phase in, for example  $\text{TiO}_2$ , have been clearly explained by Cheng *et al.* [3].

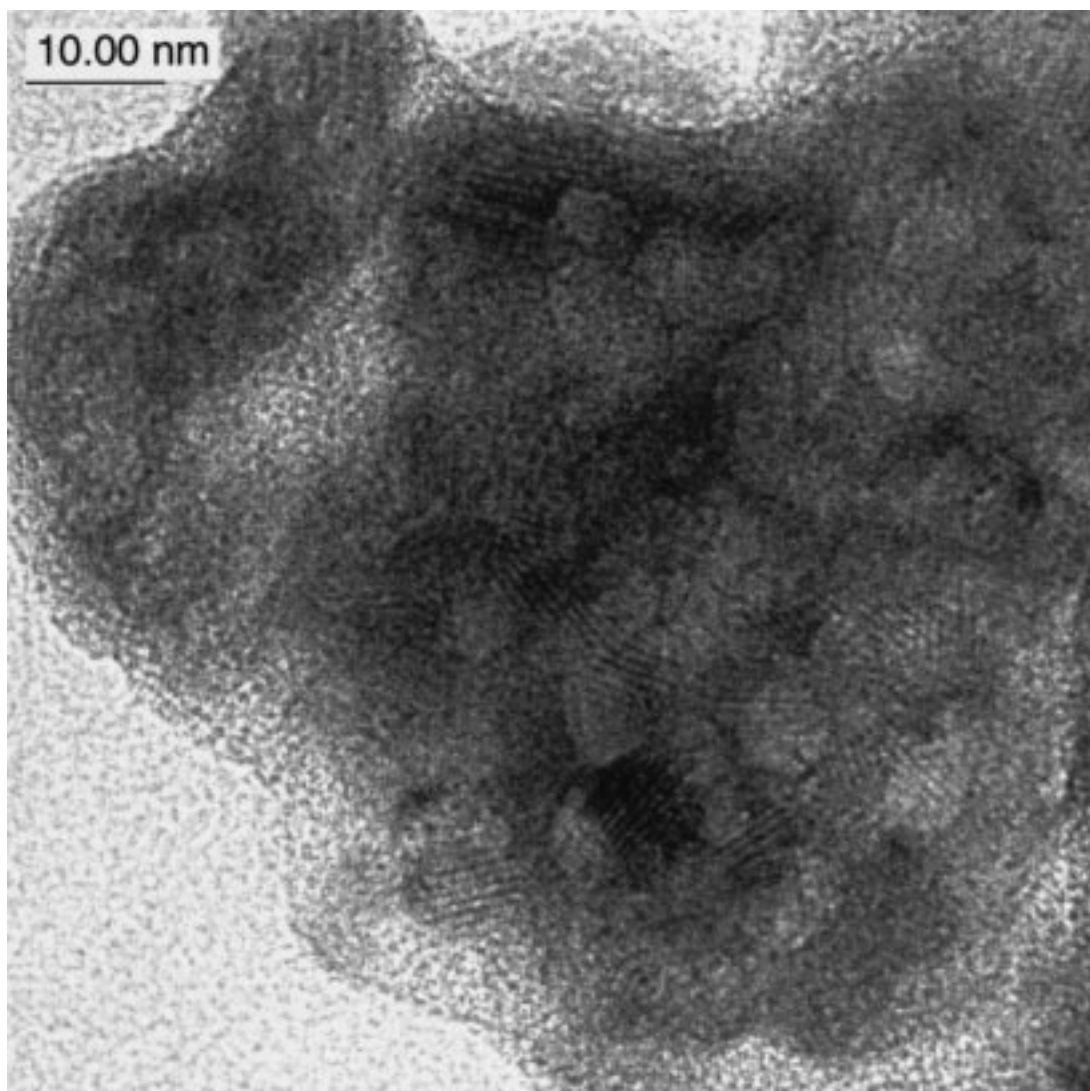


Figure 4 HRTEM micrograph on the  $\text{Y}_2\text{O}_3$  particle with spherical shape.

Seeding of particles led to an increase in transformation kinetics and to a lowering of the temperature at which the transformation from hydroxide to oxide occurs [8, 10–13]. An FTIR study of the powder obtained from precursor of yttrium chloride in the presence of a seed (Fig. 2a) revealed the presence of a weak transmittance peak at  $3300\text{ cm}^{-1}$  to  $1500\text{ cm}^{-1}$  which was attributed to the presence of water on the surface of the powder particles. This peak was found to be strong and broad in the powder obtained from yttrium nitrate as shown in Fig. 2b. However, Fig. 2a and b show the presence of peaks in the region of  $1100\text{ cm}^{-1}$  to  $1500\text{ cm}^{-1}$  which can be attributed to the presence of organic moiety from the modifier. Fig. 3 shows the evolution of the crystallite size with the hydrothermal reaction time (e.g., 1, 2 and 4 h) of the powder prepared from yttrium chloride precursor. It was found that the crystallite size increases with increase in the hydrothermal treatment time due to nucleation of the particles.

Fig. 4 shows the HRTEM micrograph of the yttria powder synthesized from yttrium chloride in the presence of a seed for 1 h. It indicates spherical morphology with a particle size  $\sim 12\text{ nm}$ . It shows  $\text{Y}_2\text{O}_3$  particles with different crystallographic orientations, which can be seen by their lattice images. The physical properties of powder obtained in the presence of a seed are given in Table I.

It can be concluded from this study that the combination of the coprecipitation and hydrothermal methods offers a promising technique for preparing

nanosize particles. Seeding plays an important role in the crystallization of yttria during the course of the hydrothermal reaction. It controls the transformation of yttrium hydroxide to yttrium oxide. It enables synthesis of yttria at a low temperature ( $\sim 190\text{ }^\circ\text{C}$ ) and produces deagglomerated particles of the yttria at lower temperature by avoiding any further calcination.

## Acknowledgments

We wish to thank Detlef Burgard of the ceramic group in the Institut fuer Neue Materialien, Saarbrücken, Germany for extensive discussions.

## References

1. Y. HIRATA and T. OZAKI, *Mater. Lett.* **15** (1992) 31.
2. D. BURGARD, C. KROPF, R. NAß and H. SCHMIDT, Better ceramic through chemistry. MRS, **346** (1994) 101.
3. H. CHENG, J. MA, Z. ZHAO and L. QUI, *Chem. Mater.* **7** (1995) 663.
4. J. T. KLOPPROGGE, J. B. H. JANSEN and J. W. GEUS, *Clays Clay Miner.* **88** (1990) 409.
5. K. YANAGISAWA, T. KUSUNOSE, K. TOKU, N. YAMASAKI, P. B. MALLA and S. KOMERNENI, *J. Mater. Sci. Lett.* **14** (1995) 1770.
6. K. YANAGISAWA, T. KUSUNOSE, K. TOKU, N. YAMASAKI, P. B. MALLA and S. KOMERNENI, *ibid.* **15** (1996) 861.
7. G. B. McGARVEY and D. G. OWEN, *J. Mater. Sci.* **31** (1996) 49.
8. L. DIAMANDESCU, D. MIHAILA-TARABASANU and N. POPESCU-POGRION, *Mater. Lett.* **27** (1996) 253.
9. S. J. WU and L. C. DeJONGHE, *J. Am. Ceram. Soc.* **79** (1996) 2207.
10. M. KUMAGAI and G. L. MESSING, *ibid.* **68** (1985) 500.
11. PRAMOD K. SHARMA, M. H. JILAVI, R. NAß, D. BURGARD and H. SCHMIDT, *ibid.* (submitted).
12. R. M. CORNELL, R. GIVANOLI and P. W. SCHINDLER, *Clay Miner.* **35** (1987) 21.
13. K. W. DYNYS and J. W. HALLORAN, in "Ultrastructure processing of ceramics, glasses and composites", edited by L. L. Hench and D. R. Ulrich (Wiley, New York, 1984) p. 142.

TABLE I Physical properties of the yttria powder

Powder characteristics	Hydrothermal treatment 190 °C for 1 h
Precursor	$\text{YCl}_3 \cdot 6\text{H}_2\text{O}$
Density	$4.99\text{ g cm}^{-3}$
Surface area (BET)	$197\text{ m}^2\text{ g}^{-1}$
Pore size	17.57 nm
Pore volume	$0.055\text{ cm}^3\text{ g}^{-1}$
Crystallite size	44 nm
Particle size	12 nm
Morphology of the particle	spherical